doi.org/10.36721/PJPS.2023.36.5.REG.1415-1424.1

Sodium p-hydroxybenzoate alleviates osteoporosis through inhibiting bone metabolism and oxidative stress via activating ERα

Xiaotian Xu, Huideng Wang, Xi Lu, Miaozhen Fan, Ailin Luo, Meng Liu, Yuhui Wang and Xiaoqun Duan*

Guangxi Colleges and Universities Key Laboratory of pharmacology, Guilin Medical University, Guilin, Guangxi, China

Abstract: As the population ages, the incidence of osteoporosis (OP) gradually increases and is becoming a growing public health problem. Meanwhile, although traditional pharmacological therapy is extremely efficient in the treatment of OP, its application is constrained because of irreversible adverse drug reactions. Therefore, scientists should actively develop safer drugs while ensuring the therapeutic effect of OP. Previous studies have shown that p-hydroxybenzoic acid (HA) can upregulate the expression of estrogen receptor (ER). Sodium p-hydroxybenzoate (DSN160) is a sodium salt of HA with a lethal dose greater than 5g/kg. However, whether DSN160 has demonstrable anti-osteoporotic activities remains unclear. In this study, DSN160 increased the organ index, length and diameter of the bone and bone mineral density and improved bone microstructure in retinoic acid-induced OP rats. Furthermore, DSN160 reduced bone metabolism-related indicators. In addition, fulvestrant (a specific antagonist of ER) blocked the anti-OP effect of DSN160. In conclusion, our findings showed that DSN160 exerts anti-OP effect through inhibiting bone metabolism and oxidative stress via activating ERα.

Keywords: Osteoporosis, sodium p-hydroxybenzoate, bone metabolism, oxidative stress, estrogen receptor α.

INTRODUCTION

Osteoporosis (OP) is the most common progressive metabolic bone disease. An imbalance in bone metabolism is considered the root of its pathogenesis. The rate of bone resorption is higher than that of bone formation with the increase in age, leading to bone loss and deterioration of bone microstructure, which increases the risk of fracture (Zhang *et al.,* 2020; Wang *et al.,* 2021). In the context of global aging population, the incidence of OP is gradually increasing, along with the increase in the number of patients with severe OP. In severe OP patients, minor falls can lead to fractures and death (Bae *et al.,* 2019; Wang *et al.,* 2020; Yong *et al.,* 2021).

Currently, the clinical drugs used for the treatment of moderate to severe OP include bisphosphonates, calcitonin, parathyroid hormone, estrogen receptor (ER) modulators, etc. However, the long-term use of these drugs may cause adverse reactions, such as allergic reactions, osteonecrosis of the jaw, acute renal failure and increased incidence of pituitary tumors (Cotts and Cifu 2018; Levin *et al.,* 2018; Leder *et al.,* 2017). Therefore, searching for a safe and effective agent that can be used to treat OP is an essential problem that remains urgent resolution. Human and veterinary researches have shown promise for a number of other natural products or compounds derived from natural sources for alleviation of arthritic symptoms (Lewis *et al.,* 2019; Liu *et al.,* 2017).

p-Hydroxybenzoic acid (HA), the active metabolite of *Nostoc commune*, up-regulates the expression of ER (sup1). Sodium p-hydroxybenzoate (DSN160) is the sodium salt form of HA and its lethal dose is greater than 5g/kg in mice, which is higher than the clinical dose. In this study, an animal model of OP induced by retinoic acid (RA) was established to explore the anti-OP effect of DSN160 and its possible mechanisms from the aspects of ER, oxidative stress and bone metabolism.

MATERIALS AND METHODS

Chemicals and reagents

DSN160 (synthesized in the laboratory at the early stage, ≥98% purity), dimethyl sulfoxide (DMSO), sodium chloride, 4% paraformaldehyde and retinoic acid (≥98% purity) were purchased from Beijing Solebo Technology Co., Ltd. Isoflurane was purchased from Shanghai Yeli Biotechnology Co., Ltd. Etidronate disodium (≥98% purity) was purchased from Shanghai Yuanye Biotechnology Co., Ltd. Calcium detection kit (96T), phosphorus detection kit (96T), superoxide dismutase (SOD) detection kit (48 T), microdermabrasion (MDA) detection kit (96T), alkaline phosphatase (ALP) detection kit (96 T) and glutathione peroxidase (GPX) detection kit (96T) were purchased from Nanjing Jiancheng Institute of Biological Engineering tartrate resistant acid phosphatase (TRACP) staining kit was purchased from Sigma.

Animals

Eight-week-old female Sprague Dawley (SD) rats (weighing 200-220g) were provided by Selleck Jingda Experimental Animal Co., Ltd. (Hunan, China). All rats were housed in an animal room at standard conditions (temperature: 21-24ºC; humidity: 45-60%; 12/12-h

*Corresponding author: e-mail: wangyuhuitg2017@163.com

light/dark cycle) and fed standard feed and water ad libitum. All animal experiments were strictly performed in accordance with the Guide for the Care and Use of Laboratory Animals, the animal approval number is GLMC201703011.

Experimental protocol

After adaptive feeding for 7 days, the rats were randomly assigned into ten groups (including two animal experiment parts) and eight rats per group. Part I: (1) Normal group; (2) RA (80mg/kg) group; (3) Etidronate disodium (Eti, 50mg/kg) group; (4) DSN160 (25mg/kg); (5) DSN160 (50mg/kg) group. Part II: (1) Normal group; (2) RA (80mg/kg) group; (3) DSN160 (50mg/kg) group; (4) Fulvestrant (25μg/kg i.p.); (5) DSN160 (50mg/kg) + Fulvestrant (25μg/kg i.p.) group. The normal group was given ultrapure water by gavage and the other groups were induced with a modeling agent (RA, 80mg/kg) for 14 days. DSN160 and Eti were administered by gavage, fulvestrant was administered by intraperitoneal injection, the corresponding drugs were given on the same day that the model was given the rats were weighed and administered according to their body weight every morning for 42 days.

Serum and urine biochemical index determination

On the last day, all rats fasted for 24h and were placed in a metabolic cage to collect urine. Then, the rats were humanely killed by cervical dislocation, blood was collected and centrifuged at 4°C and 4000rpm for 10 min to separate the serum. The levels of calcium, phosphorus, SOD, MDA, GPX and ALP in the serum and the levels of calcium and phosphorus in urine of rats were determined following the kit's instructions (Nanjing Jiancheng Bioengineering Institute, Nanjing, Jiangsu, China).

Measurement of Organ Coefficients

The uterus and ovaries of each rat were collected and weighed. The femur and tibia of the rats were collected. The externally adhered tissues, such as meat and tendons, were removed with a blade and the bone marrow was retained and finally weighed. The organ coefficients were calculated according to the following formula: organ coefficient=organ weight/body weight×100.

Bone Quality Assays

After collecting the lumbar vertebrae (L1) and measured the length and width of the femur and L1 with an electronic vernier caliper. The rat femur samples were immersed in phosphate buffered saline (PBS) at room temperature. Micro CT (ZKKS-MCT-Sharp) was used to determine the BMD of the sample in two-dimensional (2D) and the microstructure parameters of bone which include total bone volume (BV/TV), trabecular bone thickness (Tb.Th) and trabecular bone separation (Tb.Sp) in three-dimensional (3D). Scanning parameter settings source voltage: 70kVp; source current: 100μA; exploration time: 70ms.

Haematoxylin and eosin (H&E) staining

The rat femur samples were fixed in 10% buffered formalin for 24h. After washing 3 times with PBS, bone tissues were decalcified with ethylenediaminetetraacetic acid (EDTA) for one month. Tissues were then routinely dehydrated, embedded and cut into 5μm decalcified sections. After dewaxing and hydration, the sections were stained with H&E. Lastly, sections were dehydrated, cleared and sealed with neutral balsam and the pathological characteristics were observed under an optical microscope.

Tartrate-resistant acid phosphatase (TRACP) staining assay

After the paraffin-embedded sections were deparaffinized and hydrated, they were stained with TRACP and observed on a BX43 microscope (Olympus). The nucleus was stained blue. The positive expression of TRACP was expressed as bright or deep red granules occurred in the cytoplasm. All the giant cells with TRACR-positive expression containing 3 or more nucleus were considered as osteoclasts. Five fields of view were randomly selected to calculate the number of osteoclasts.

Quantitative real-time PCR (qRT-PCR) assay

Total RNA was isolated from the femur with TRIzol reagent (Invitrogen). And quantified using a NanoDrop 2000 spectrophotometer (Thermo Fisher Scientific Inc., Waltham, Massachusetts, USA). The total RNA was transcribed into cDNA by using a transcriptor reverse transcriptase. The cDNA was used as the template, the CFX96 fluorescent quantitative PCR instrument was used to perform genetic testing under the conditions of 95°C for 10 s and 60°C for 30s to detect the mRNA expression of ERα. Expressions of the target genes were carried out by a comparative method ($2^{-\Delta\Delta Ct}$) using GAPDH as an internal reference. The primer pairs used are shown in table 1.

STATISTICAL ANALYSIS

The experimental data were analyzed using GraphPad Prism v.8.02 (GraphPad Software, Lajolla, CA, USA). Data were expressed as mean ± standard error of the mean (SEM). Student's t-test was used for comparison between two groups and One-way ANOVA was used for comparison between multiple groups. $P<0.05$ was considered statistically significant.

Table 1: Primer sequence

Genes	Primer (5'-3')
GAPDH-F	GACATGCCGCCTGGAGAAAC
GAPDH-R	AGCCCAGGATGCCCTTTAGT
ERα-F	GCCGCCTTCAGTGCCAACAG
ERα-R	GGCTCGTTCTCCAGGTAGTAGGG

RESULTS

DSN160 attenuated RA-induced OP in rats

To explore the effect of DSN160 on RA-induced OP, we intragastrically administered DSN160 to the OP rats, with Eti as a positive control. The results showed that oral RA treatment slowed down the weight gain (fig. 1A) and weight loss of femur and tibia (fig. 1B) in the rats. Compared with the normal control group, the vertebra and femur diameter and length also significantly reduced in the model group (figs. 1C-1F). Micro-computed tomography bone imaging displayed that compared with the normal control group, the bone mineral density decreased and the bone microstructure deteriorated in the model group (figs. 2A-2F). Moreover, hematoxylin and eosin (H&E) staining showed that in the model group, the number of femoral trabeculae was reduced (fig. 2G). The weight of rats in the DSN160 (50mg/kg) group reached in the fourth week, consistent with the normal group. In addition, DSN160 can significantly increase the weight of femur and tibia, the diameter and length of femur and vertebrae, bone density and the number of trabeculae and significantly improve the bone microstructure. All these findings showed that DSN160 can evidently inhibit OP in RA-induced rats.

The balance between osteoblasts and bone resorption osteoclasts plays a key role in maintaining bone remodeling (Kim *et al.,* 2017). Osteoclasts are multinucleated cells formed by autolysis of monocytes and macrophages and they can develop and adhere to the bone matrix. They degrade the bone matrix by secreting acid and lyase to induce bone loss and induce OP (Chen *et al.,* 2018; Ono and Nakashima 2018). To explore the effect of DSN160 on osteoclasts, the changes in osteoclasts were observed by tartrate-resistant acid phosphatase staining. The results showed that the number of osteoclasts in the femur of the model group significantly increased compared with that in the normal group (fig. 3) and that of osteoclasts in the femur of OP rats significantly reduced after DSN160 treatment. The above findings showed that DSN160 improved OP through inhibition of osteoclast formation.

In this study, the organ indexes of rat ovary and uterus were measured. The results showed that DSN160 considerably protected against reduced organ indexes of ovary and uterus in OP rats (figs. 4A-4B). H&E staining showed that the uterine cavity of the model group was enlarged compared with the normal group. After the administration of DSN160, the uterine cavity of OP rats was significantly reduced, especially in the DSN160 (50mg/kg) group (fig. 4C).

DSN160 inhibited bone metabolism and oxidation in OP rats

Further, we evaluated the effect of DSN160 on bone metabolism corresponding to the blood and urine markers in OP rats. The results showed that calcium, phosphorus and alkaline phosphatase (ALP) in the serum of OP rats and calcium and phosphorus in the urine significantly increased compared with those of the normal group (figs. 5A-5E). After the administration of DSN160, the serum calcium, phosphorus and ALP and the calcium and phosphorus in the urine significantly reduced. DSN160 (50mg/kg) almost caused the calcium, phosphorus and ALP concentrations to return to normal levels. In addition, to investigate the effect of DSN160 on oxidative stress, we measured the oxidation level in the rat serum. The results showed that the level of malondialdehyde (MDA) in OP rats increased and those of glutathione peroxidase (GPX) and superoxide dismutase (SOD) decreased significantly compared with the normal group. In addition, the results showed that the MDA levels were suppressed and the GPX and SOD levels were promoted after DSN160 treatment of OP rats (figs. 5F-5H). DSN160 (50mg/kg) can almost reduce the serum MDA, GPX and SOD levels and induce their return to normal levels. The above findings showed that DSN160 can improve OP by regulating oxidative stress and bone metabolism. Notably, the improved effect of DSN160 on oxidative stress and bone metabolism was closely related to its protection against experimental OP (Yao *et al.,* 2020; Qin *et al.,* 2019).

DSN160 alleviated op in rats through inhibiting bone metabolism and oxidative stress via activating ERα

To determine whether ERα plays a key role in DSN160 anti-OP, we determined the expression level of ERα in femur by quantitative reverse-transcription polymerase chain reaction. As shown in fig. 6, compared with the normal group, the expression level of ERα in the model group significantly reduced, but the expression level of ERα can be significantly increased under DSN160 treatment.

Subsequently, to further study the role of ERα in inhibiting OP by DSN160, we continuously injected fulvestrant intraperitoneally. The data showed that fulvestrant attenuated the effects of DSN160 on increasing OP rats body weight, femur and tibia weight, femur and vertebra diameter and length (figs. 7A-7F), increased bone density and the number of trabeculae, improved bone microstructure (figs. 8A-8G) and inhibited the formation of osteoclasts (figs. 9A and 9B). We determined whether DSN160 inhibits bone metabolism and oxidative stress in an ERα-dependent manner to improve OP. A kit was used to measure the expression levels of calcium, phosphorus, ALP, MDA, GPX and SOD in the serum and calcium and phosphorus in the urine. The data showed that fulvestrant significantly weakened the effect of DSN160 on reducing calcium, phosphorus and ALP concentrations (figs. 10A-10E). In addition, fulvestrant significantly weakened the effect of DSN160 on reducing MDA expression and increasing GPX and SOD expression (figs. 10F-10H). Thus, DSN160 can increase bone density and improve OP by

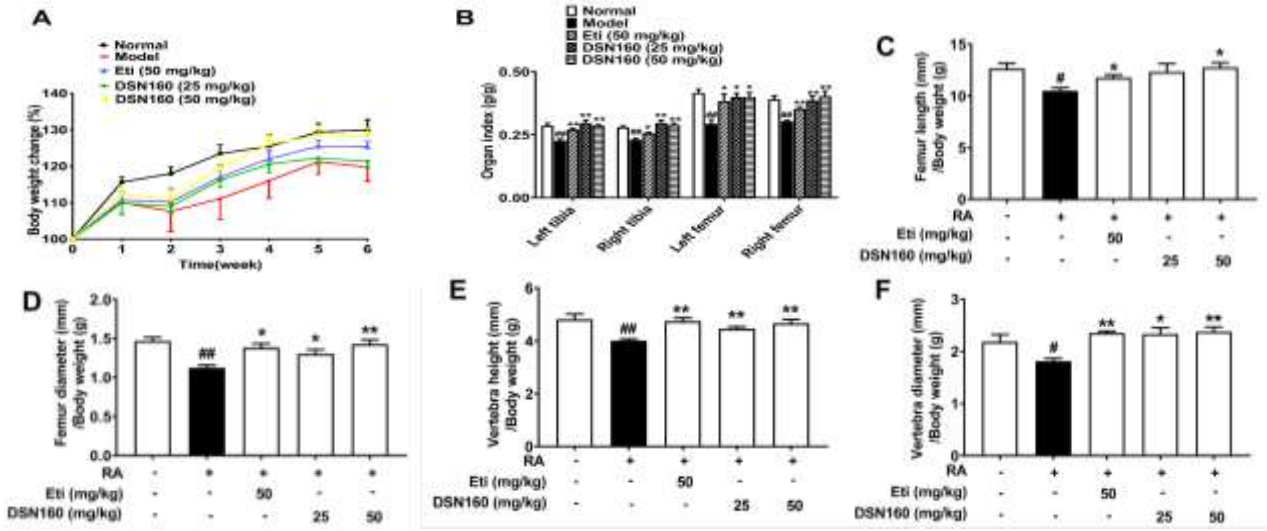

Fig. 1: Effects of DSN160 on RA induced OP. Except for normal group, rats in other groups were given RA gavage for 14 consecutive days, while DSN160 (25, 50mg/kg) and etidronate disodium (Eti) (50mg/kg) were gavaged for 42 days. (A) Changes in body weight. (B) Changes in organ indexes of femur and tibia. (C-F) Changes in femur length, femur diameter, vertebral height and vertebral diameter. Data was represented by means ± SEM, n=8. $^{\#}P<0.05$, $^{\#\#}P<0.01$ *vs.* normal group. $^{*}P<0.05$. $^{**}P<0.01$ *vs.* RA group.

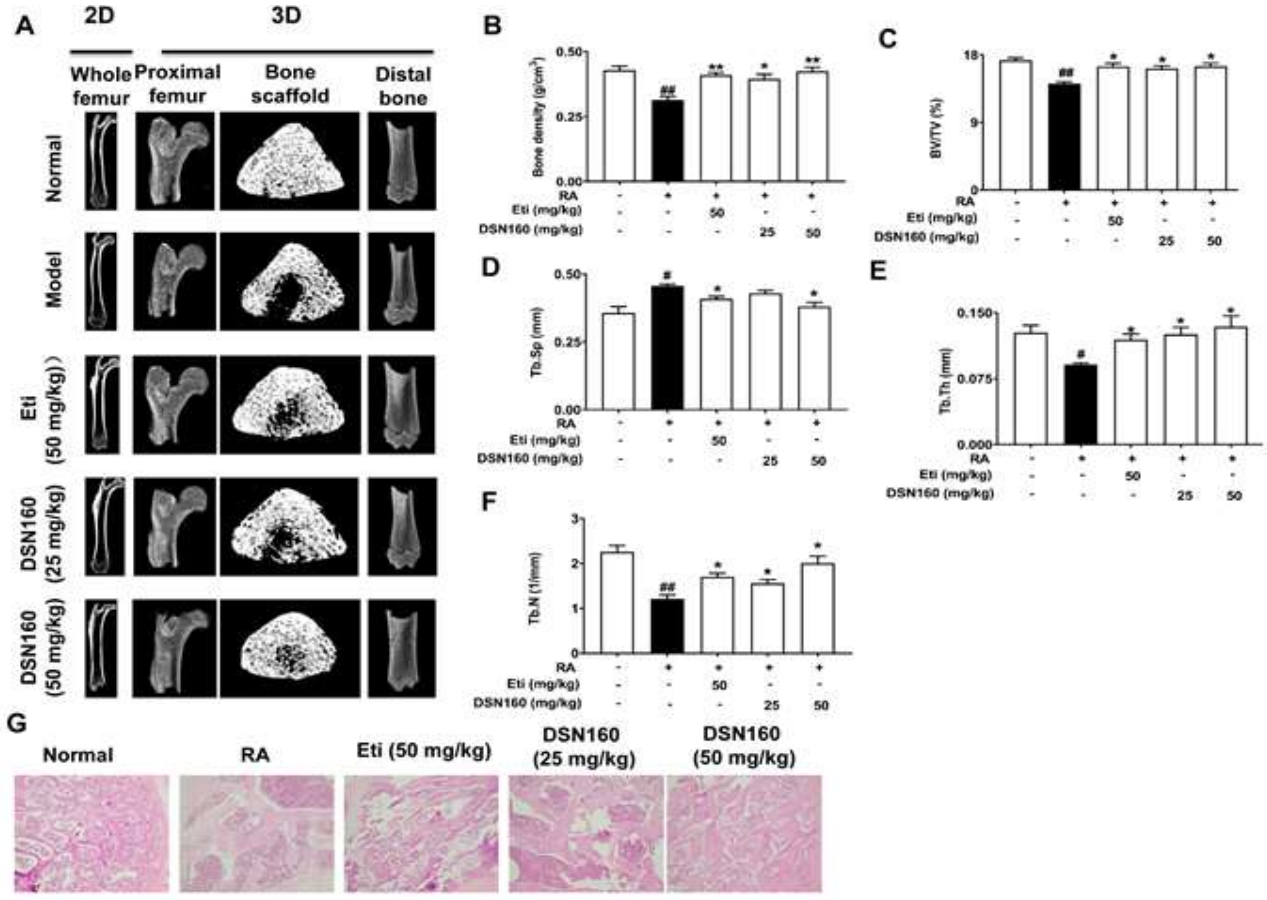

Fig. 2: The effect of DSN160 on OP bone density and bone microstructure. (A) Micro CT inspection results. (B) BMD. (C-F) BV/TV, Tb.Sp, Tb.Th and Tb.N. (G) Femoral H&E staining results. Data was expressed as mean±SEM, n=8. $^{\#}P<0.05$, $^{\#\#}P<0.01$ *vs*. normal group. $^{*}P<0.05$. $^{**}P<0.01$ *vs*. RA group.

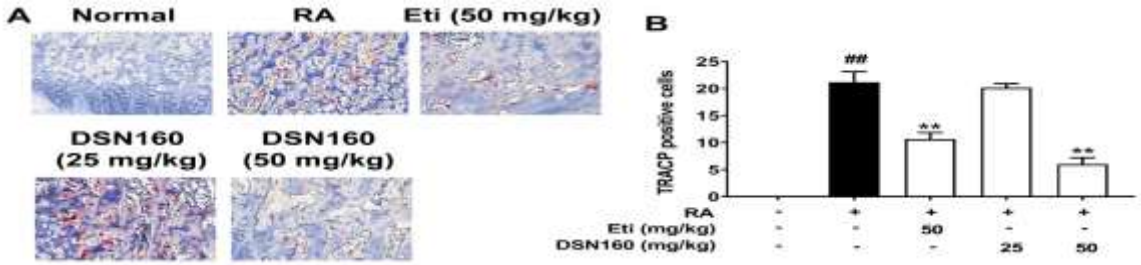

Fig. 3: The effect of DSN160 on the formation of osteoclasts in the femur of OP rats. (A-B) TRAP staining of femoral osteoclasts. Data was expressed as mean ± SEM, n=8. $^{\#\#}P<0.01$ *vs*. normal group. $^{**}P<0.01$ *vs*. RA group.

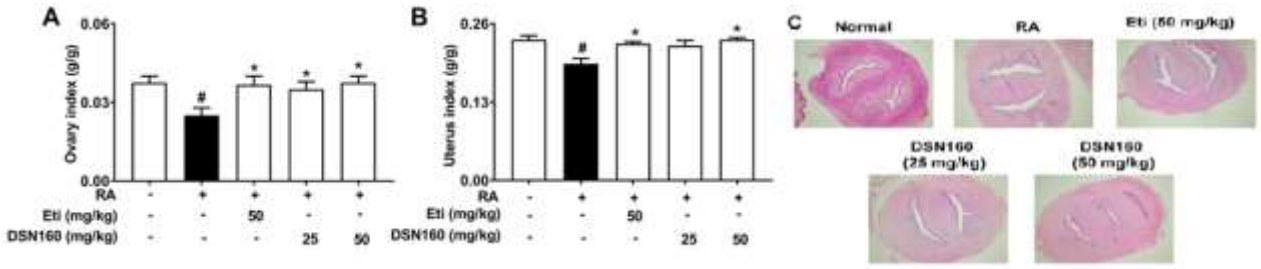

Fig. 4: The effect of DSN160 on the reproductive organs of OP rats. (A) Ovarian organ index. (B) Uterine organ index. (C) Uterine pathological changes (40×). Data was expressed as mean ± SEM, n=8. $^{\#}P<0.05$ *vs*. normal group. $^{*}P<0.05$ *vs*.

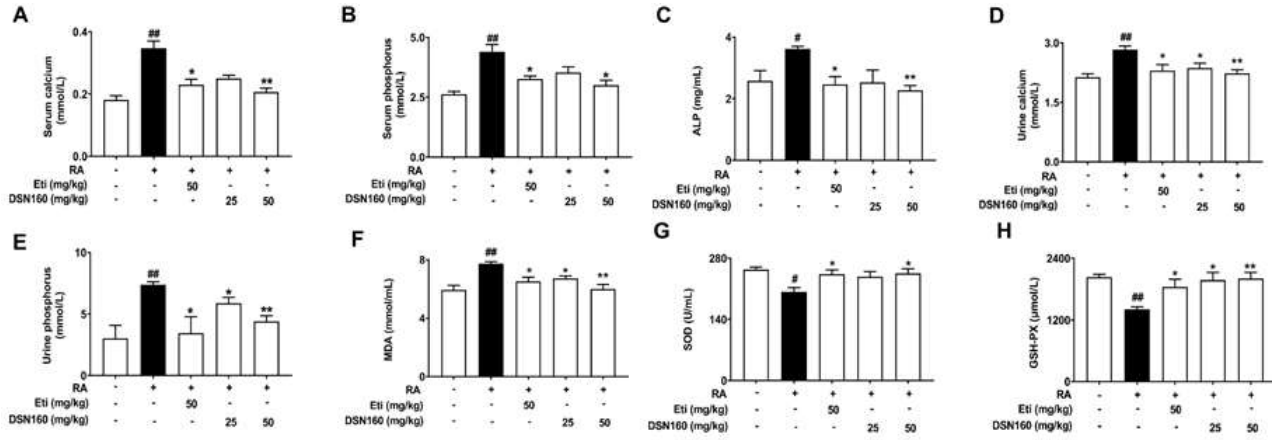

Fig. 5: The effect of DSN160 on bone metabolism and the expression of oxidative markers in OP rats. The content of (A) serum calcium, (B) serum phosphorus, (C) serum ALP, (D) urine calcium, (E) urine phosphorus, (F) serum MDA, (G) serum SOD and (H) serum GSH-PX were detected by using the kit. Data was represented by means ± SEM, n=8. $^{\#}P<0.05$, $^{\#\#}P<0.01$ *vs*. normal group. $^{*}P<0.05$. $^{**}P<0.01$ *vs*. RA group.

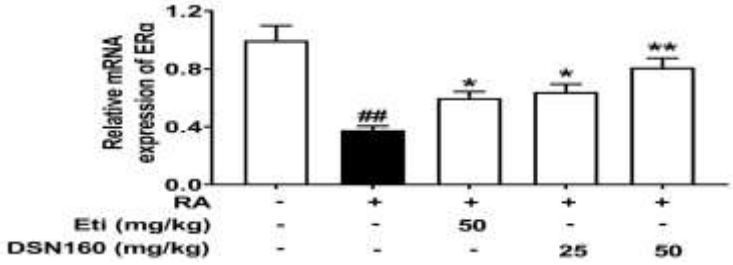

Fig. 6: The effect of DSN160 on the expression of ERα in the femur of OP rats. The expression of ERα in the femur was detected by qRT-PCR. Data was represented by means ± SEM, n=8. $^{\#\#}P<0.01$ *vs*. normal group. $^{*}P<0.05$. $^{**}P<0.01$ *vs*. RA group.

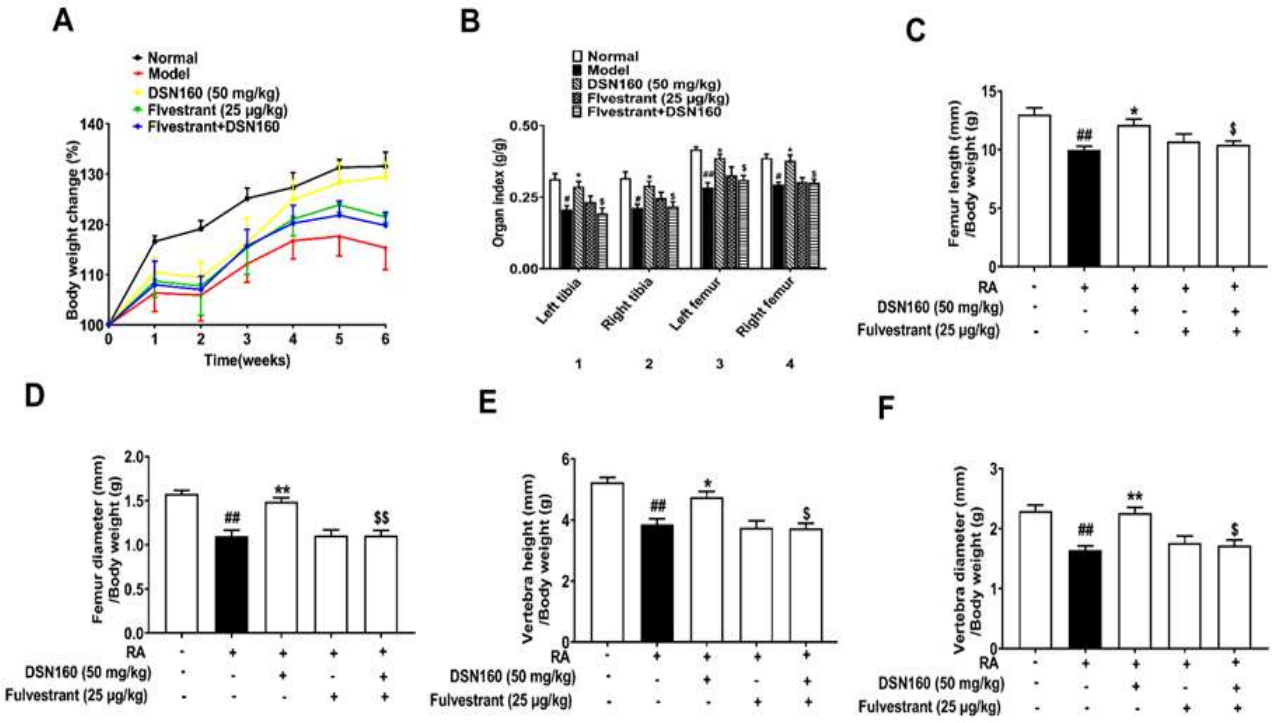

Fig. 7: The effect of fulvestrant in DSN160 on the tibia, femur and vertebrae of RA-induced OP rats. Rats were fed RA for 14 days, orally DSN160 (50 mg/kg) and intraperitoneal injection of fulvestrant (25μg/kg) for 42 consecutive days. (A) Changes in body weight. (B) Changes in organ indexes of femur and tibia. (C-F) Changes in femur length, femur diameter, vertebral height and vertebral diameter. Data was represented by means ± SEM, n=8. $^{\#}P<0.05$, $^{\#\#}P<0.01$ *vs.* normal group. $^{*}P<0.05$. $^{**}P<0.01$ *vs.* RA group. $^{\$}P<0.05$. $^{\$\$}P<0.01$ *vs.* DSN160 (50mg/kg) group.

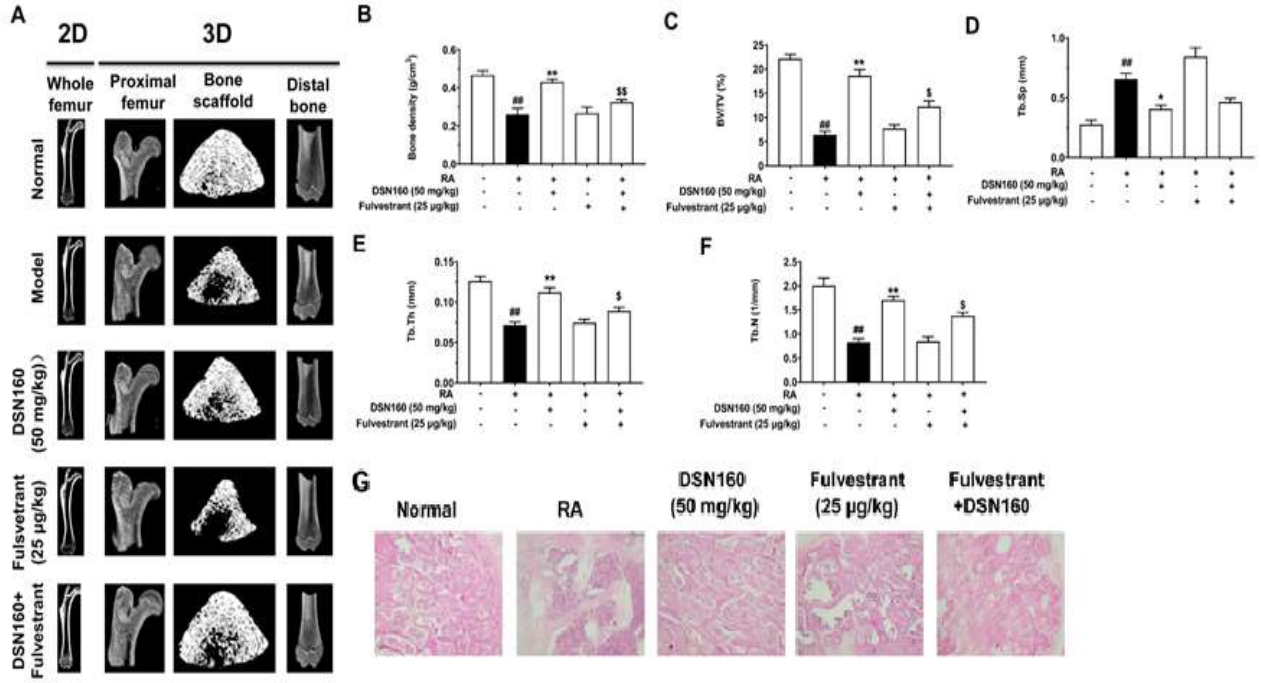

Fig. 8: The effect of fulvestrant in DSN160 on bone mineral density, bone microstructure and trabecular bone in RA-induced OP rats. (A) Micro CT inspection results. (B) BMD. (C-F) BV/TV, Tb. Sp, Tb. Th and Tb. N. (G) Femoral H&E staining results (40×). Data was represented by means ± SEM, n=8. $^{\#\#}P<0.01$ *vs.* normal group. $^{*}P<0.05$. $^{**}P<0.01$ *vs.* RA group. $^{\$}P<0.05$. $^{\$\$}P<0.01$ *vs.* DSN160 (50mg/kg) group.

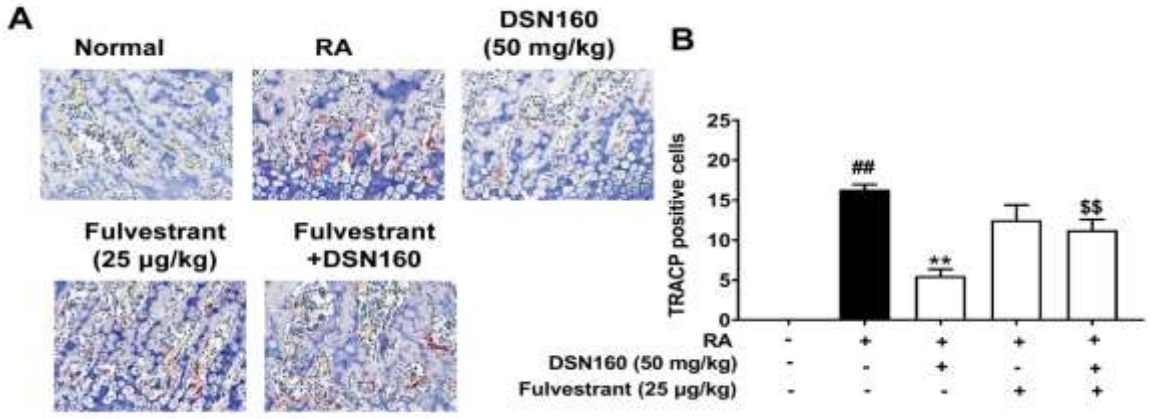

Fig. 9: The effect of fulvestrant in DSN160 on the formation of femoral osteoclasts in OP rats. (A-B) TRAP staining of femoral osteoclasts. Data was expressed as mean ± SEM, n=8. $^{\#\#}P<0.01$ *vs*. normal group. $^{**}P<0.01$ *vs*. RA group. $^{\$\$}P<0.01$ *vs*. DSN160 (50mg/kg) group.

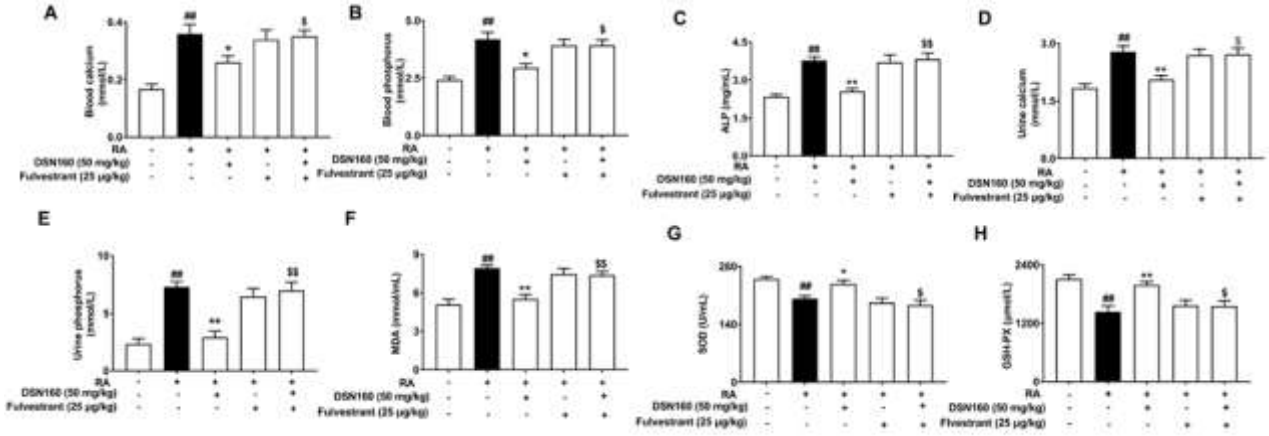

Fig. 10: The effect of fulvestrant in DSN160 on the expression of bone metabolism and oxidation markers in OP rats. Use of (A) serum calcium, (B) serum phosphorus, (C) serum ALP, (D) urine calcium, (E) urine phosphorus, (F) serum MDA, (G) serum SOD and (H) serum GSH-PX Kit detection. Data was expressed as mean ± SEM, n=8. $^{\#\#}P<0.01$ *vs*. normal group. $^{*}P<0.05$. $^{**}P<0.01$ *vs*. RA group. $^{\$}P<0.05$. $^{\$\$}P<0.01$ *vs*. DSN160 (50mg/kg) group.

activating ERα and inhibiting bone metabolism and oxidative stress.

DISCUSSION

OP is a common chronic bone disease (Wang *et al.*, 2020). Once it develops to the advanced stage, the fracture incidence and mortality increase significantly. Thus, OP has become a global epidemic (Liu *et al.*, 2022; Wang *et al.*, 2021).

The etiology and pathogenesis of OP may be associated with bone metabolism imbalance and oxidative stress (Chen *et al.*, 2018; Wang *et al.*, 2021; Compston *et al.*, 2019). Multiple studies have demonstrated that interventions aimed at improving one or more of these factors have the potential to relieve OP significantly (Krishnan and Muthusami 2017; Chen *et al.*, 2019). Previous studies have shown that compounds obtained from plants have potential protective or therapeutic effects on OP (Zhang *et al.*, *2020*; Xie *et al.*, 2021; He *et al.*, 2019). For example, Boswellic acid attenuated the disease symptoms of experimental OP through improving bone metabolism (Al-Dhubiab *et al.*, 2020). Melatonin ameliorated RA-induced OP through regulating bone metabolism and inhibiting oxidative stress in model mic (Wang *et al.*, 2021). Similarly, in this study, DSN160 can increase the diameter and length of rat vertebrae and femurs by regulating bone metabolism and inhibiting oxidative stress, improving bone microstructure and increasing bone density and the number of bone trabeculae to inhibit RA-induced OP.

Calcium and phosphorus are essential bone minerals for all animals and play important roles in numerous physiological processes including bone metabolism (Al-Dhubiab *et al.*, 2020). An evidence indicates that OP patients have higher levels of calcium and phosphorus in

the serum and urine than healthy controls (Zhang *et al.,* 2020; Li *et al.,* 2018). Similarly, this phenomenon has been verified in the animal model of RA-induced OP (Liu *et al.,* 2020). In addition, ALP is an important indicator of bone metabolism (Sun *et al.,* 2020), and it can degrade a variety of phosphonates in an alkaline environment and has the function of transferring phosphate groups. In bone tissue, ALP is only synthesized and secreted by osteoblasts, whereas it is involved in the calcification of bone matrix (Vimalraj 2020; Brady *et al.,* 2019; Orsolic *et al.,* 2018; Liu *et al.,* 2022). The serum ALP level significantly increased in OP patients and RA-induced animal models, but the level of serum ALP decreased significantly after therapy (Zhuang *et al.,* 2020). Melatonin can improve RA-induced OP in animal models through inhibiting the increase in serum ALP and reduce the concentrations of calcium and phosphorus in the serum and urine (Wang *et al.,* 2021). Our study revealed that the levels of calcium and phosphorus in the urine and serum and the level of ALP in the serum decreased significantly after the administration of DSN160 in RA-induced OP rats. Thus, DSN160 can treat OP by inhibiting bone metabolism.

Oxidative stress plays an important role in bone formation (Qin *et al.,* 2019). The excessive generation and accumulation of free radicals can induce oxidative stress and cause lipid peroxidation, inhibit osteogenic differentiation and promote bone resorption (Qin *et al.,* 2019; Kimball *et al.,* 2021). SOD and GPX are important antioxidant substances and their activities reflect indirectly the ability of organisms to remove oxygen-free radicals (Gusti *et al.,* 2021; Kimball *et al.,* 2021). MDA is the final decomposition product of lipid peroxidation and its content can reflect the speed and intensity of lipid peroxidation in tissue cells (Chen *et al.,* 2020; Tsikas 2017). Studies have shown that MDA was significantly elevated in the serum of postmenopausal women with OP, whereas SOD and GPX were conversely. The original glycosides of *Epimedium* extract can improve the oxidative stress of bones by improving the antioxidant enzyme activity and antioxidant capacity of OP rats (Xi *et al.,* 2019). This study showed that DSN160 reversed the downward trend of SOD and GPX contents in the model, showing a strong potential for the removal of peroxide products. This result indicated that DSN160 can resist OP by improving the oxidative stress state of bones.

The cells of bone tissue contain E (Ho *et al.,* 2018). ERα is transcription factor involved in the regulation of numerous complex physiological processes in humans and plays an important role in several pathological processes including OP (Hamilton *et al.,* 2017; Cai *et al.,* 2021). ERα can inhibit bone resorption by inducing osteoclast apoptosis and mounting evidence shows that decreased ERα expression is one of the reasons for OP (Saoji *et al.,* 2019; Cai *et al.,* 2021). Huang Kui *et al.* observed that psoralen can up-regulate the expression of ERα in the OVX group to promote fracture healing (Huang *et al.,* 2018). Luna Ge *et al*. reported that isopsoralen can promote osteoblast differentiation by increasing the expression of ERα, thereby improving the symptoms of OP (Ge *et al.,* 2018). In this study, RA reduced the expression of ERα in rat femurs. However, after the administration of DSN160, the expression of ERα increased and the OP symptoms of rats significantly improved. In addition, the antagonist fulvestrant significantly weakened the improvement effect of DSN160 on bone metabolism and oxidative stress, which indicates that the improvement effect of DSN160 on bone metabolism and oxidative stress in OP rats depended on ERα.

CONCLUSION

In conclusion, our research revealed that DSN160 exerts anti-OP effects through inhibiting bone metabolism and oxidative stress via activating ERα. Therefore, we suggest that DSN160 can be used as a new compound to prevent OP due to its anti-OP effect.

ACKNOWLEDGMENTS

This work was supported by the National Natural Science Foundation of China (82160615), the Natural Science Foundation of Guangxi (2017GXNSFBA198104, 2018GXNSFAA138098, 2019GXNSFBA245104), the special funding for 2017 Guangxi BaGui Scholars and Guangxi science and technology base and talent special fund (gui ke AD19110123, gui ke AD18281016).

REFERENCES

Al-Dhubiab BE, Patel SS, Morsy MA, Duvva H, Nair AB, Deb PK and Shah J (2020). The beneficial effect of boswellic acid on bone metabolism and possible mechanisms of action in experimental osteoporosis. *Nutrients*, **12**(10): 3186.

Almeida M and Porter RM (2019). Sirtuins and FoxOs in osteoporosis and osteoarthritis. *Bone*, **121**: 284-292.

Bae IS, Kim JM, Cheong JH, Han MH and Ryu JI (2019). Association between cerebral atrophy and osteoporotic vertebral compression fractures. *PlosOne*, **14**(11): E0224439.

Brady JJ, McGoldrick D, O'Callaghan K, McNamara F, Mulready KJ, Cullen MR, Denieffe S and Fitzgibbon M (2019). Bone alkaline phosphatase on the IDS-iSYS automated analyser; cross-reactivity with intestinal ALP. *Clin. Chem. Lab. Med.,* **57**(8): e186-e188.

Cai XY, Zhang ZJ, Xiong JL, Yang M and Wang ZT (2021). Experimental and molecular docking studies of estrogen-like and anti-osteoporosis activity of compounds in *Fructus psoraleae. J. Ethnopharmacol*., **276**: 114044.

Chen L, Wang G, Wang Q, Liu Q, Sun Q and Chen L (2019). N-acetylcysteine prevents orchiectomy-induced osteoporosis by inhibiting oxidative stress and osteocyte senescence. *Am. J. Transl Res*., **11**(7): 4337-4347.

Chen X, Wang Z, Duan N, Zhu G, Schwarz EM and Xie C (2018). Osteoblast-osteoclast interactions. *Connect Tissue. Res*., **59**(2): 99-107.

Chen Y, Li YQ, Fang JY, Li P and Li F (2020). Establishment of the concurrent experimental model of osteoporosis combined with Alzheimer's disease in rat and the dual-effects of echinacoside and acteoside from Cistanche tubulosa. *J. Ethnopharmacol*., **257**: 112834.

Compston JE, McClung MR and Leslie WD (2019). Osteoporosis. *Lancet*, **393**(10169): 364-376.

Cotts KG and Cifu AS (2018). Treatment of osteoporosis. *JAMA*., **319**(10): 1040-1041.

Ge L, Cui Y, Cheng K and Han J (2018). Isopsoralen enhanced osteogenesis by targeting AhR/ERα. *Molecules*, **23**(10): 2600.

Gusti AMT, Qusti SY, Alshammari EM, Toraih EA and Fawzy MS (2021). Antioxidants-Related Superoxide Dismutase (SOD), Catalase (CAT), Glutathione Peroxidase (GPX), Glutathione-S-Transferase (GST), and Nitric Oxide Synthase (NOS) gene variants analysis in an obese population: A preliminary case-control study. *Antioxidants (Basel*), **10**(4): 595.

He J, Li X, Wang Z, Bennett S, Chen K, Xiao Z, Zhan J, Chen S, Hou Y, Chen J, Wang S, Xu J and Lin D. (2019). Therapeutic anabolic and anticatabolic benefits of natural Chinese medicines for the treatment of osteoporosis. *Front. Pharmacol*., **10**(25): 1344.

Ho MX, Poon CC, Wong KC, Qiu ZC and Wong MS (2018). Icariin, but not genistein, exerts osteogenic and anti-apoptotic effects in osteoblastic cells by selective activation of non-genomic ERα signaling. *Front. Pharmacol*., **9**: 474.

Huang K, Sun YQ, Chen XF, Tian F, Cheng F, Gong QL and Liu KB (2018). Psoralen, a natural phytoestrogen, improves diaphyseal fracture healing in ovariectomized mice: A preliminary study. *Exp. Ther.Med*., **21**(4): 368.

Hamilton KJ, Hewitt SC, Arao Y and Korach KS (2017). Estrogen hormone biology. *Curr. Top. Dev. Biol*., **125**: 109-146.

Kim JH, Kim M, Jung HS and Sohn Y (2019). *Leonurus sibiricus* L. ethanol extract promotes osteoblast differentiation and inhibits osteoclast formation. *Int. J. Mol. Med.*, **44**(3): 913-926.

Kimball JS, Johnson JP and Carlson DA (2021). Oxidative stress and osteoporosis. *J. Bone. Joint. Surg. Am*., **103**(15): 1451-1461.

Krishnan A and Muthusami S (2017). Hormonal alterations in PCOS and its influence on bone metabolism. *J. Endocrinol*., **232**(2): R99-R113.

Leder BZ (2017). Parathyroid hormone and parathyroid hormone-related protein analogs in osteoporosis therapy. *Curr. Osteoporos. Rep*., **15**(2): 110-119.

Levin VA, Jiang X and Kagan R (2018). Estrogen therapy for osteoporosis in the modern era. *Osteoporos. Int*., **29**(5): 1049-1055.

Lewis R, Gómez Alvarez CB, Rayman M, Lanham-New S, Woolf A and Mobasheri A (2019). Strategies for optimising musculoskeletal health in the 21st century. *BMC. Musculoskelet. Disord*., **20**(1): 164.

Li W, Zhu HM, Xu HD, Zhang B and Huang SM (2018). CRNDE impacts the proliferation of osteoclast by estrogen deficiency in postmenopausal osteoporosis. *Eur. Rev. Med. Pharmacol. Sci*., **22**(28): 5815-5821.

Liu C, Ma R, Wang L, Zhu R, Liu H, Guo Y, Zhao B, Zhao S, Tang J, Li Y, Niu J, Fu M, Zhang D and Gao S (2017). Rehmanniae radix in osteoporosis: A review of traditional Chinese medicinal uses, phytochemistry, pharmacokinetics and pharmacology. *J. Ethnopharmacol*., **198**: 351-362.

Liu X, Fan JB, Hu J, Li F, Yi R, Tan F and Zhao X (2020). *Lactobacillus fermentum* ZS40 prevents secondary osteoporosis in Wistar Rat. *Food. Sci. Nutr*., **8**(9): 5182-5191.

Liu H, Zhao A, Huang Y, Hou A, Miao W, Hong L, Deng N and Fan Y(2022). Efficacy and mechanisms of oleuropein in postmenopausal osteoporosis. *Comput. Math. Methods Med*., **2022**: 9767113.

Nash LA and Ward WE (2017). Tea and bone health: Findings from human studies, potential mechanisms, and identification of knowledge gaps. *Crit. Rev. Food. Sci. Nutr*., **57**(8): 1603-1617.

Ono T and Nakashima T (2018). Recent advances in osteoclast biology. *Histochem. Cell Bio*., **149**(4): 325-341.

Orsolic N, Jelec Z, Nemrava J, Balta V, Gregorovic G and Jelec D (2018). Effect of quercetin on bone mineral status and markers of bone turnover in retinoic acid-induced osteoporosis. *Pol. J. Food. Nutr. Sci*., **68**(2): 149-162.

Qin D, Zhang H, Zhang H, Sun T, Zhao H and Lee WH (2019). Anti-osteoporosis effects of osteoking via reducing reactive oxygen species. *J. Ethnopharmacol*., **244**: 112045.

Saoji R, Desai M, Das RS, Das TK and Khatkhatay MI (2019). Estrogen receptor α and β gene polymorphism in relation to bone mineral density and lipid profile in Northeast Indian women. *Gene*. **710**: 202-209.

Sun Y, Chen R, Zhu D, Shen ZQ, Zhao HB and Lee WH (2020). Osteoking improves OP rat by enhancing HSP90-β expression. *Int. J. Mol. Med*., **45**(5): 1543-1553.

Tarawneh A, Taqvi S, Salem K and Sahota O (2020). Cervical spine fragility fractures in older people: 5-year experience at a regional spine centre. *Age Ageing*, **49**(6): 1102-1104.

Tsikas D (2017). Assessment of lipid peroxidation by measuring malondialdehyde (MDA) and relatives in biological samples: Analytical and biological challenges. *Anal. Biochem*. **524**: 13-30.

Vimalraj S (2020). Alkaline phosphatase: Structure, expression and its function in bone mineralization. *Gene*, **754**: 144855.

Wang X, Ji Q, Hu W, Zhang Z, Hu F, Cao S, Wang Q, Hao Y, Gao M and Zhang X (2021). Isobavachalcone prevents osteoporosis by suppressing activation of ERK and NF-κB pathways and M1 polarization of macrophages. *Int. Immunopharmaco*., **94**: 107370.

Wang QF, Bi HS, Qin ZL, Wang P, Nie FF and Zhang GW (2020). Associations of LRP5 gene with bone mineral density, bone turnover markers and fractures in the elderly with osteoporosis. *Front*. *Endocrinol* (*Lausanne*), **11**: 571549.

Wang X, Liang T, Zhu Y, Qiu J, Qiu X, Lian C, Gao B, Peng Y, Liang A, Zhou H, Yang X, Liao Z, Li Y, Xu C, Su P and Huang D (2021). Correction to Melatonin prevents bone destruction in mice with retinoic acid-induced osteoporosis. *Mol. Med*., **25**(1): 43.

Wang XJ, Liu JW and Liu J (2020). MiR-655-3p inhibits the progression of osteoporosis by targeting LSD1 and activating BMP-2/Smad signaling pathway. *Hum. Exp. Toxicol*., **39**(10): 1390-1404.

Xi Y, Jiang T, Yu J, Xue M, Xu N, Wen J, Wang W, He H and Ye X (2019). Preliminary studies on the anti-osteoporosis activity of Baohuoside I. *Biomed. Pharmacother*., **115**: 108850.

Xie CL, Park KH, Kang SS, Cho KM and Lee DH (2021). Isoflavone-enriched soybean leaves attenuate ovariectomy-induced osteoporosis in rats by anti-inflammatory activity. *J. Sci. Food. Agric*., **101**(4): 1499-1506.

Yao D, Huang L, Ke J, Zhang M, Xiao Q and Zhu X (2020). Bone metabolism regulation: Implications for the treatment of bone diseases. *Biomed. Pharmacother*., **129**: 110494.

Zhang Z, Zhao Q, Liu T, Zhao H, Wang R, Li H, Zhang Y, Shan L, He B, Wang X, Huang L, Hao D and Sun H (2020). Effect of Vicenin-2 on ovariectomy-induced osteoporosis in rats. *Biomed. Pharmacother*., **129**: 110474.

Yong EL and Logan S (2021). Menopausal osteoporosis: Screening, prevention and treatment. *Singapore. Med. J.*, **62**(4):159-166.

Zhuang Y, Sun X, Liu B, Hou H and Sun Y (2020). Effects of Rambutan Peel (*Nephelium lappaceum*) Phenolic extract on RANKL-induced differentiation of RAW264.7 cells into osteoclasts and retinoic acid-induced osteoporosis in rats. *Nutrients*, **12**(4): 883.